

# Phase-modulated radio over fiber multimode links

Ivana Gasulla<sup>1,2,\*</sup> and José Capmany<sup>1</sup>

<sup>1</sup>*ITEAM Research Institute, Universidad Politécnica de Valencia, Camino de Vera s/n, 46022 Valencia, Spain*

<sup>2</sup>*Currently with the Edward L. Ginzton Laboratory, Stanford University, 348 Via Pueblo Mall, Stanford, California 94305, USA*

\*[igasulla@stanford.edu](mailto:igasulla@stanford.edu)

**Abstract:** We present the first experimental demonstration of a phase-modulated MMF link implementing high-frequency digital transmission in a cost-effective solution based on direct detection. Successful subcarrier transmission of QPSK, 16-QAM and 64-QAM data channels for bit rates up to 120 Mb/s through a 5 km MMF link is achieved over the microwave region comprised between 6 and 20 GHz. The overall capacity of the proposed approach can be further increased by properly accommodating more passband channels in the operative frequency range determined by the phase-to-intensity conversion process provided by the dispersive nature of the optical fiber. In this sense, our results show the possibility of achieving an aggregate bit rate per length product of 144 Gb/s·km and confirm, in consequence, the possibility of broadband phase-modulated radio over fiber transmission through MMF links suitable for multichannel SCM signal distribution.

©2012 Optical Society of America

**OCIS codes:** (060.2330) Fiber optics communications; (060.2360) Fiber optics links and subsystems; (060.5060) Phase modulation; (060.5625) Radio frequency photonics.

---

## References and links

1. H. R. Stuart, "Dispersive multiplexing in multimode optical fiber," *Science* **289**(5477), 281–283 (2000).
2. M. G. Larrode, A. M. J. Koonen, J. J. V. Olmos, and A. Ng'Oma, "Bidirectional radio-over-fiber link employing optical frequency multiplication," *IEEE Photon. Technol. Lett.* **18**(1), 241–243 (2006).
3. R. Shah, R. C. J. Hsu, A. Tarighat, A. H. Sayed, and B. Jalali, "Coherent optical MIMO (COMIMO)," *J. Lightwave Technol.* **23**(8), 2410–2419 (2005).
4. E. J. Tyler, P. Kourtessis, M. Webster, E. Rochart, T. Quinlan, S. E. M. Dudley, S. D. Walker, R. V. Pentyl, and I. H. White, "Toward terabit-per-second capacities over multimode fiber links using SCM/WDM techniques," *J. Lightwave Technol.* **21**(12), 3237–3243 (2003).
5. J. M. Tang, P. M. Lane, and K. A. Shore, "Transmission performance of adaptively modulated optical OFDM signals in multimode fiber links," *IEEE Photon. Technol. Lett.* **18**(1), 205–207 (2006).
6. I. Gasulla and J. Capmany, "1 Tb/s x km multimode fiber link combining WDM transmission and low-linewidth lasers," *Opt. Express* **16**(11), 8033–8038 (2008).
7. P. Hartmann and A. Xin Qian, Wonfor, R. V. Pentyl, and I. H. White, "1–20 GHz directly modulated radio over MMF link," in *Proceedings of IEEE Microwave Photonics MWP2005*, (Seoul, South Korea, 2005), 95–98.
8. I. Gasulla and J. Capmany, "High-frequency radio over fibre QPSK transmission through a 5 km multimode fibre link," in *Proceedings of 33rd European Conference on Optical Communication*, (Berlin, Germany, 2007), 2 pp.
9. D. H. Sim, Y. Takushima, and Y. C. Chung, "Transmission of 10-Gb/s and 40-Gb/s signals over 3.7 km of multimode fiber using mode-field matched center launching technique," in *Proceedings of Optical Fiber Communication Conference 2007*, (Anaheim, USA, 2007), OTuL3.
10. V. J. Urlick, F. Bucholtz, P. S. Devgan, J. D. McKinney, and K. J. Williams, "Phase modulation with interferometric detection as an alternative to intensity modulation with direct detection for analog-photonics links," *IEEE Trans. Microw. Theory Tech.* **55**(9), 1978–1985 (2007).
11. H. Chi, X. Zou, and J. Yao, "Analytical models for phase-modulation-based microwave photonic systems with phase modulation to intensity modulation conversion using a dispersive device," *J. Lightwave Technol.* **27**(5), 511–521 (2009).
12. D. Marpaung, C. Roeloffzen, A. Leinse, and M. Hoekman, "A photonic chip based frequency discriminator for a high performance microwave photonic link," *Opt. Express* **18**(26), 27359–27370 (2010).

13. M. J. LaGasse and S. Thaniyavaru, "Bias-free high-dynamic-range phase-modulated fiber-optic link," *IEEE Photon. Technol. Lett.* **9**(5), 681–683 (1997).
14. J. Zhang and T. E. Darcie, "Low-biased microwave-photonic link using optical frequency or phase modulation and fiber-Bragg-grating discriminator," in *Proceedings of Optical Fiber Communication Conference*, (Anaheim, USA, 2006), OWG1.
15. J. M. Wyrwas and M. C. Wu, "Wu," "Dynamic range of frequency modulated direct-detection analog fiber optic links," *J. Lightwave Technol.* **27**(24), 5552–5562 (2009).
16. T. E. Darcie, J. Zhang, P. F. Driessen, and J.-J. Eun, "Class-B microwave-photonic link using optical frequency modulation and linear frequency discriminators," *J. Lightwave Technol.* **25**(1), 157–164 (2007).
17. I. Gasulla and J. Capmany, "Transfer function of multimode fiber links using an electric field propagation model: Application to Radio over Fibre Systems," *Opt. Express* **14**(20), 9051–9070 (2006).
18. I. Gasulla and J. Capmany, "Analytical model and figures of merit for filtered Microwave Photonic Links," *Opt. Express* **19**(20), 19758–19774 (2011).
19. D. Visani, G. Tartarini, M. N. Petersen, L. Tarlazzi, and P. Faccin, "Link design rules for cost-effective short-range radio over multimode fiber systems," *IEEE Trans. Microw. Theory Tech.* **58**(11), 3144–3153 (2010).
20. G. Alcaro, D. Visani, L. Tarlazzi, P. Faccin, and G. Tartarini, "Distortion mechanisms originating from modal noise in radio over multimode fiber links," *IEEE Trans. Microw. Theory Tech.* **60**(1), 185–194 (2012).
21. R. A. Shafik, S. Rahman, and A. Islam, "On the extended relationships among EVM, BER and SNR as performance metrics," in *Proceedings of International Conference on Electrical and Computer Engineering*, (Dhaka, Bangladesh, 2006), 408–411.
22. I. Gasulla and J. Capmany, "Analysis of the harmonic and intermodulation distortion in a multimode fiber optic link," *Opt. Express* **15**(15), 9366–9371 (2007).
23. I. Gasulla and J. Capmany, "Simultaneous baseband and radio over fiber signal transmission over a 5 km MMF link," in *Proceedings of IEEE Microwave Photonics MWP2008*, (Goald Coast, Australia, 2008), 209–212.

---

## 1. Introduction

The increasing transmission capacity demand following the 10-Gigabit Ethernet standard in access and in-building networks has been fuelling dynamic research on different techniques directed to the improvement of the transmission bandwidth in the existing multimode optical fibre (MMF) infrastructure. MMFs are present in many in-building networks and some middle reach 1-10 km access networks and there is an important drive to overcome their inherent intermodal dispersion with a means of exploiting them for broadband transmission. A wide range of contributions, including mode group diversity multiplexing [1], optical frequency multiplication [2], the application of MIMO (Multiple Input Multiple Output) techniques [3], subcarrier multiplexing (SCM) [4], Orthogonal Frequency-Division Multiplexing (OFDM) [5] and wavelength division multiplexing (WDM) [4,6], are trying to accomplish this goal implementing intensity modulated radio over fiber (ROF) transmission with either direct or coherent detection schemes. On the other hand, the use of low linewidth lasers, instead of traditional LED based transmitters, has been demonstrated to support the delivery of ROF signals beyond the typical MMF bandwidth-distance product [7,8] for a range of microwave frequencies up to 20 GHz through MMF links up to 5 km. Actually, the combination of mode-filtering solutions implemented by centrally launching the light from a SMF, and low linewidth lasers has shown the capability of reaching broadband transmission, both radio over fibre [7,8] and digital baseband [6,9] transmission, in middle-reach MMF links.

Up to date, all the approaches oriented to enhance the transmission bandwidth in MMF networks were based on conventional intensity modulated (IM) architectures. However, phase modulation microwave photonic (PM-MWP) links can bring many advantages in comparison with IM links since phase modulators can provide a higher degree of linearity and do not require active bias control circuitry [10–14]. In addition, multichannel systems can benefit from less crosstalk due to nonlinearities when applying constant-intensity phase modulation (PM) while improvements on the noise level or system linearity can be achieved by properly designing the optical filter discriminator required for phase-to-intensity conversion in some PM-MWP architectures. While traditional demodulation systems were based on coherent detection or feedback loops, the search for simplified phase-to-intensity conversion solutions employing square-low photodetectors has recently led to the proposal of the inclusion of dispersive devices as Fiber Bragg gratings [14], post-modulation optical carrier filtering, balanced [10] or unbalanced [13] interferometric detection systems, as well as optical

frequency discriminators for dynamic range enhancement in either frequency [15,16] or phase modulated [12] links. Although the implementation of these techniques in access networks results in a potential cost reduction, a deeper reduction in complexity can be achieved if we take advantage of the frequency response of phase modulated 2nd-order dispersive fiber links derived from the carrier suppression effect (CSE) at regions far from baseband [11].

We therefore propose a cost-effective PM-MWP link employing direct detection in which the effect of the chromatic dispersion on the double sideband characteristic of the modulated signal allows broadband passband digital transmission through a middle-reach MMF link provided that low-linewidth lasers are used and central launching is implemented. The technique is thus especially suited for access networks where the fiber presents enough chromatic dispersion to avoid the requirement of a frequency discriminator prior to optical detection. In this paper we report, for the first time to our knowledge, the experimental demonstration of high-frequency digital radio signal transmission at bit rates up to 120 Mb/s in a PM-MWP link comprising a 5 km 62.5- $\mu\text{m}$  core-diameter graded-index silica MMF link.

## 2. Experimental results and discussion

The scheme of the setup for the experimental demonstration of subcarrier digital channels transmission is depicted in Fig. 1. A vector signal generator generates the radiofrequency (RF) carriers which can be modulated by quadrature phase shift keying (QPSK) or multilevel quadrature amplitude modulation (16-QAM and 64-QAM) data channels at bit rates up to 120 Mb/s. The subcarrier frequency was varied between 1 and 20 GHz, while the electrical modulating power was set to 15 dBm. The combined RF signal is used to externally modulate the phase of the optical signal generated by the tunable distributed feedback (DFB) laser emitting 3.10 dBm at a wavelength of 1560 nm. The phase modulated optical carrier is then central launched from a 9- $\mu\text{m}$  core-diameter SMF by means of an FC/PC connector into a 5 km dispersive link implemented with 62.5- $\mu\text{m}$ -core diameter silica graded-index (parabolic core grading) MMF with an standard first order chromatic dispersion parameter of  $D = 17$  ps/(nm·km). The SM-MM launch scheme provides an initial spatial filtering effect by launching only a limited number of low-order modes into the MMF. After detection using a MMF-pigtailed 23-GHz-bandwidth PIN photodiode, the electrical signal passed through a 30-dB RF amplifier with a 40 GHz bandwidth before being properly demodulated by a signal analyzer (20 Hz - 26.5 GHz) with a maximum demodulation bandwidth of 25 MHz.

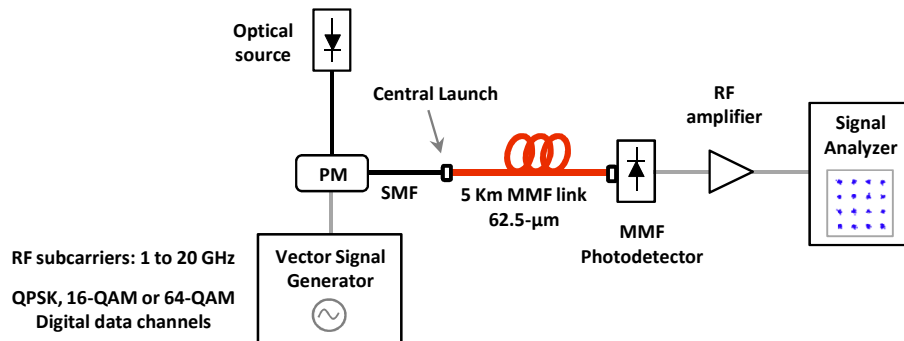


Fig. 1. Experimental setup.

The potential of MMFs for broadband ROF transmission has been demonstrated for IM links as a consequence of the nonideal behavior as a microwave transversal photonic filter of the MMF [17], where reduction of the inherent intermodal dispersion can be achieved thanks to the combination of low-linewidth sources (such as DFB lasers) and central light injection.

On the other hand, theoretical justification on the possibility of implementing PM direct detection links, relies on the transmission of microwave subcarriers properly located at the

passband regions placed between the frequency notches that the CSE produces on the RF gain link response which are due to the phase offset between the upper and lower modulation sidebands [18]. In fact, the closed-form expressions for the main figures of merit applicable to general PM-MWP systems were developed in [18] and subsequently particularized to 2nd-order dispersive PM MMF links with single-detection architecture. By expanding the propagation constant  $\beta(\omega)$  in a Taylor's series around the central angular frequency  $\omega_0$

$$\beta(\omega) \approx \beta(\omega_0) + \left. \frac{d\beta(\omega)}{d\omega} \right|_{\omega=\omega_0} (\omega - \omega_0) + \frac{1}{2} \left. \frac{d^2\beta(\omega)}{d\omega^2} \right|_{\omega=\omega_0} (\omega - \omega_0)^2 = \beta^0 + \beta^1(\omega - \omega_0) + \frac{1}{2} \beta^2(\omega - \omega_0)^2 \quad (1)$$

and considering an optical source represented by a Gaussian power spectrum with a root-mean square (RMS) linewidth  $\Delta W$

$$P_s(\omega) = P_0 \frac{\sqrt{\pi}}{\Delta W} e^{-\frac{\omega^2}{(2\Delta W)^2}}, \quad (2)$$

the formula for the RF end-to-end link gain can be derived as

$$G_{RF}^\Phi(\Omega) = (4I_{dc}\pi/V_\pi)^2 R_{in}R_{out} e^{-2(\beta_0^2 L \Omega \Delta W)^2} \sin^2(\beta_0^0 \Omega^2 L / 2) \left| \sum_{m=1}^M 2m(C_{mm} + G_{mm}) e^{-\alpha_m^0 L} e^{-j\tau_m \Omega} \right|^2 \quad (3)$$

where  $I_{dc}$  is the DC photocurrent at the link output,  $V_\pi$  is the modulator quadrature voltage while  $R_{in}$  and  $R_{out}$  are the respective input and output resistances. We can observe that the first exponential factor is a low-pass frequency response term which depends on  $\beta_0^2$  and  $\Delta W$ , while the intermediate sinusoidal factor is the well-known carrier suppression effect. This sinusoidal factor represents a PM to IM conversion efficiency, which limits the minimum length of application. If  $f_{min} = \Omega_{min} / 2\pi$  represents the minimum frequency to be transmitted, then assuming a minimum conversion efficiency of  $-20$  dB (electrical) results in  $L \geq 0.1 / (2\pi^2 \beta_0^2 f_{min}^2)$ . As an example, for the typical values  $\beta_0^2 = -21$  psec<sup>2</sup>/km and  $f_{min} = 10$  GHz used in the reported measurements,  $L \geq 2.41$  km, which is within the range of access networks. The last term, which comprises a summation between all the propagated mode groups, represents a microwave photonic transversal filtering effect whose samples correspond to different mode groups. Each sample  $m$  is time delayed by the modal group delay  $\tau_m$  [17], and has an amplitude which depends on the modal attenuation  $\alpha_m^0$  and the sum of the light injection coefficient  $C_{mm}$  (see Eq. (5) of [17]) and the modal-coupling coefficient  $G_{mm}$  defined for power transitions between adjacent mode groups (see Eq. (77) of [17]).

In order to confirm the results obtained in [18] and previous to the passband digital transmission, we measured the electrical frequency response of the PM MMF link for frequencies up to 30 GHz employing a network analyzer. Figure 2(a) shows both the measured and theoretical results (computed from (3)) for the 5 km MMF link as well as the measured spectra of eight photodetected SCM channels ranging from 1 to 20 GHz when performing digital transmission. As an example, we include in Fig. 2(b) an inset detailing the spectrum corresponding to a 6-MHz-span zoom over the 1 GHz subcarrier for 1 Mb/s QPSK transmission. The measured frequency response has been calibrated in order to isolate both the phase modulator (20 GHz) and the detector (23 GHz) 3-dB RF bandwidth limitations from the MMF link response.

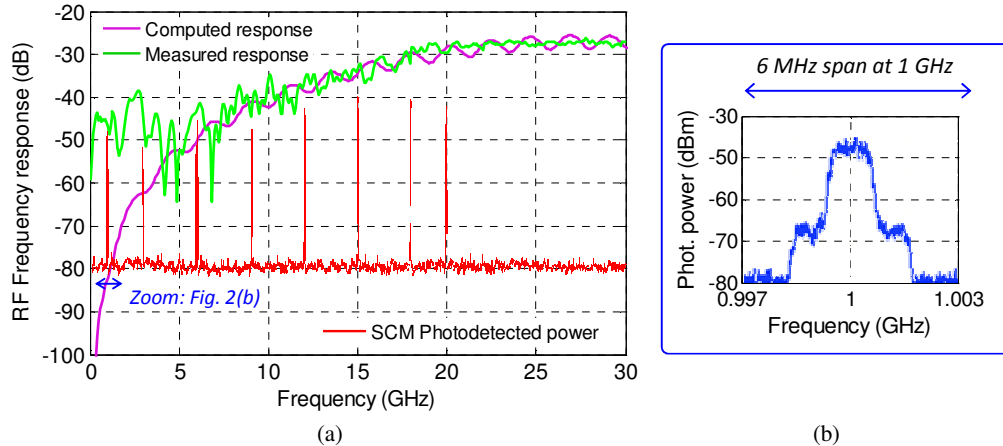


Fig. 2. (a) Measured and computed RF link frequency response and measured spectra of the photodetected SCM signals. (b) 6-MHz-span zoom of the channel over 1 GHz for 1 Mb/s QPSK transmission.

The computation of the MMF transversal filtering effect described in Eq. (3) assumes a selective central assignment of the light injection coefficient  $C_{mm}$  where the three lowest-order mode groups have been excited following a pronounced Gaussian distribution, where the first mode group contains around the 80% of the injected energy. The concentration of most of the energy in the axial core region subsequently reduces the effect of modal dispersion from the coupling of the high-order modes to the lower ones [18]. It must be noted that a total number of  $M = 10$  mode groups are propagated through the MMF at 1560 nm.

We can see a mismatch between theoretical and experimental results in the baseband region. In theory a notch due to the CSE should be present which is smoothed due to the time average of fluctuations in the MMF response. In fact, the transmission performance of the evaluated link is subject to the appearance of modal noise as a consequence of the temporal statistical nature of the speckle pattern at the MMF output when launching a highly coherent light. It can be affirmed that modal noise is induced when the MMF link contains a combination of the following conditions: a sufficiently narrow laser spectrum in conjunction with mode-selective losses (such as microbending), source frequency fluctuations and time-varying fiber disturbances. Moreover, the effect of modal noise can be increased if some form of spatial filtering is present at the output, such as misaligned fiber joints and connectors. In practice, it has been found that for direct-modulation RoF systems modal noise contributes to fluctuations in the RF gain [19] and, as recently found [20], to nonlinear distortion. However, progress in the quality of optical connector technology can lead to a significant reduction of its impact. For PM modulation a similar behavior is expected which could be confirmed by carrying a similar analysis as in [20]. In this case one should expect a more robust behavior against nonlinearities since phase modulation is inherently linear.

The measured response for this case confirms that the PM-MMF link is, in principle, suitable for passband channel stable transmission above 6-7 GHz. Measured Error Vector Magnitude (EVM) values illustrated below show that this a conservative estimation as the usable spectral region can be increased in the lower region of the RF spectrum.

With the purpose of evaluating the impact of the electrical subcarrier frequency on the quality of the demodulated signal, we analysed the digital space constellations of the measured In-phase/Quadrature polar vector for the channel frequencies of 1, 3, 6, 9, 12, 15, 18 and 20 GHz. The EVM is a common quality metric widely used in digital communication systems that relates the performance of the actual waveform compared to an ideal signal as calculated over the course of the ideal constellation. The resorted signal analyzer provides the RMS value of the EVM over time at the instants of the symbol clock transitions:

$$EVM(\%) = \sqrt{\frac{P_{error}}{P_{reference}}} \cdot 100\% \quad (4)$$

where  $P_{error}$  is the RMS power of the error vector and  $P_{reference}$  is the RMS power of the ideal transmitted signal. Here the maximum IEEE 802.11 allowed EVM values of 12.5% for QPSK, 11.2% for 16-QAM and 5.6% for 64-QAM data are assumed as standard criteria for signal quality evaluation.

Figure 3 plots the RMS EVM values, averaged over time, measured for 10, 20 and 40 Mb/s QPSK, 20, 40 and 80 Mb/s 16-QAM while 30, 60 and 120 Mb/s 64-QAM encoding formats versus the subcarrier radiofrequency. In general, as predicted by the phase-to-intensity conversion curve illustrated in Fig. 1(b), the EVM increases at lower frequencies. In case of QPSK we can appreciate that a good signal quality is obtained for the whole frequency range as the EVM is always well below the standard 12.5%, with values below 5% for 20 Mb/s. For 16-QAM and 64-QAM modulations, the highest values, respectively around 14% and 8%, were achieved at one of the lowest frequencies (3 GHz) where, in fact, the major fluctuations of the MMF link response are encountered. In these cases, the channel frequencies comprised between 12 and 20 GHz show, especially at high bit rates, the best signal quality as expected from the high-pass filtering characteristic of the dispersive fiber link.

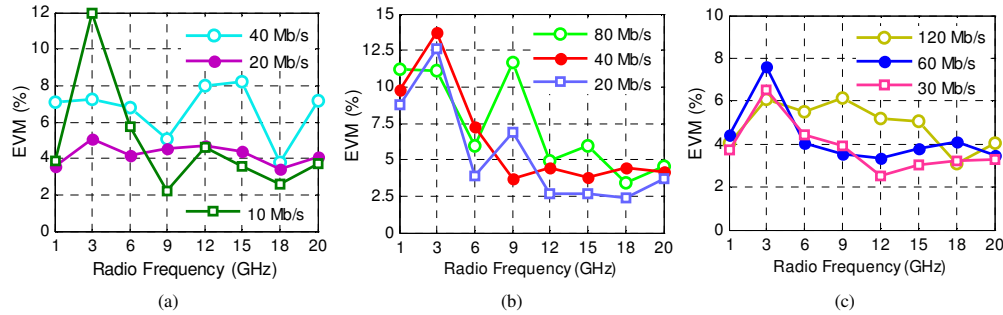


Fig. 3. Measured EVM (%) versus electrical subcarrier frequency for (a) QPSK, (b) 16-QAM and (c) 64-QAM modulation.

The measured constellation diagrams for the determined high-frequency subcarrier region are depicted in Fig. 4 for the three modulation formats under consideration when selecting the higher achieved bit rate for every format, which actually corresponds to a symbol rate of 20 Ms/s. In that case, both the 16-QAM and 64-QAM symbols mostly concentrated well around the reference constellation, while for QPSK a slightly more scattered pattern was obtained, in line with the EVM evaluation shown in Fig. 3. Note that a considerable better location of the QPSK constellation points was reached when decreasing the bit rate down to 20 Mb/s or 10 Mb/s, again in full agreement with the measured EVM. Even so, a good location of the constellation points was achieved in every high-frequency subcarrier for the maximum bit rate transmission. This result relates, in the worst-case scenario, to a minimum signal-to-noise ratio (SNR) of 21.9 dB (maximum EVM of 8%) for QPSK, while 24.6 dB (maximum EVM of 5.9%) for 16-QAM and 25.8 dB (maximum EVM of 5.1%) for 64-QAM, since  $SNR \approx 1 / (EVM^2)$  [19]. The bit error rate (BER) can be actually related to the measured RMS EVM by applying the following equation for a general  $M$ -ary modulation system [19],

$$P_b \approx \frac{2(1-1/L)}{\log_2 L} Q \left[ \sqrt{\left( \frac{3 \log_2 L}{L^2 - 1} \right) \frac{2}{EVM^2 \log_2 M}} \right], \quad (5)$$

where  $L$  represents the number of levels in each dimension of the  $M$ -ary modulation format and  $Q$  is the Gaussian co-error function. The evaluation of Eq. (5) allows us to corroborate that error-free transmission has been successfully demonstrated since the measured EVM figures are translated into computed BER values well below  $10^{-15}$  and  $10^{-12}$  respectively for QPSK and 16-QAM modulations, while around  $10^{-6}$  for 64-QAM, which, if required, could be improved by properly applying error correction coding.

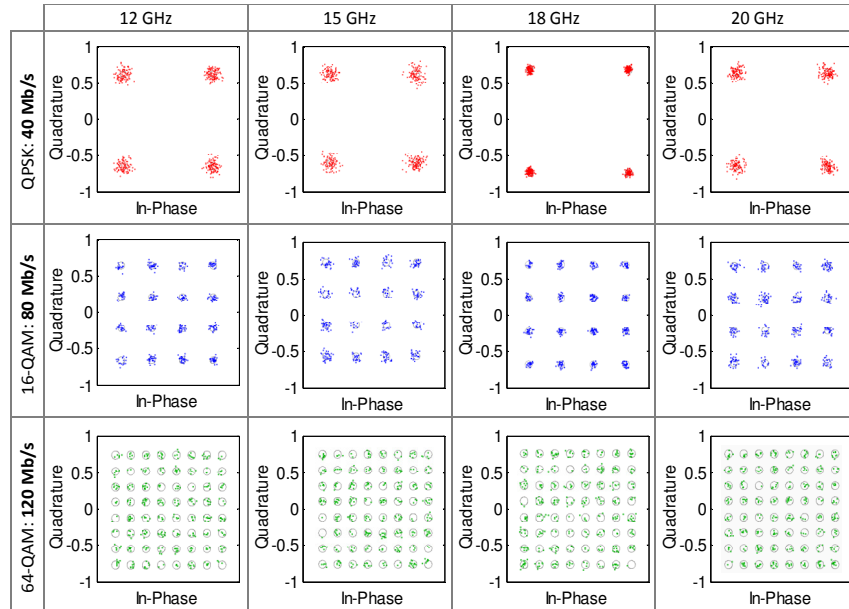


Fig. 4. Measured constellation diagrams for different modulation formats and bit rates at the subcarrier channel frequencies ranging from 12 to 20 GHz.

### 3. Practical considerations

Although the reported results were computed for the case of independent single subcarrier transmission they nevertheless show the possibility of further increasing the total capacity if more channels are accommodated in the operative microwave region determined by the phase-to-intensity conversion process. Figure 5 depicts a schematic of the proposed multichannel SCM signal distribution. The modification of the evaluated experimental setup in order to consider simultaneous transmission, i.e. real implementation of subcarrier multiplexing (SCM), would require taking into account the harmonic and intermodulation distortion arisen in the system. An estimate of the impact of these sources of impairment has been provided in a previous work by the authors [22,23], where the evaluation of the impact of second and third order distortions through the analysis of the Composite Second Order (CSO) and the Composite Triple Beat (CTB) parameters showed the potential feasibility of implementing subcarrier modulation techniques in MMF links. In particular and referring to the case depicted in Fig. 5, the possible nonlinearities due to the RF multiplexing stage and subsequent modulation circuitry should be limited or compensated to avoid them from becoming a dominant source of impairment. Under those conditions, the theoretical analysis carried out in [22] showed that for an application case as the one reported in this paper, (typical modulation index value of  $m = 0.01$  as well as usual fiber parameters), the distortion will have a negligible impact in ROF transmission with high requirements ( $CSO < -50$  dBc).

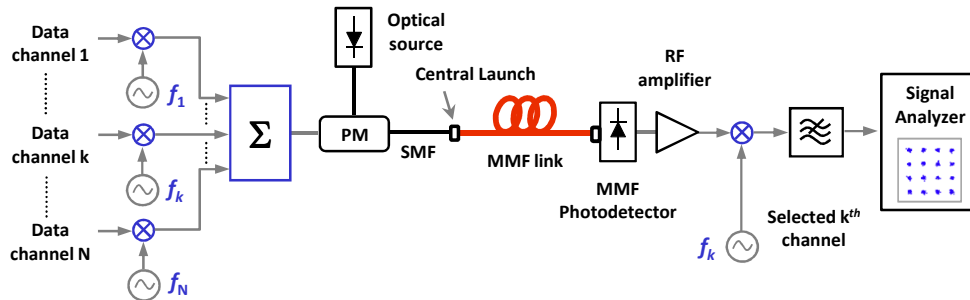


Fig. 5. Multichannel SCM signal distribution in the proposed phase-modulated MMF link.

Also, as it has been previously mentioned, a more complete analysis including the impact of modal noise on the system nonlinearities could be carried by adapting the model developed in [20] to the specific case of external phase modulation. Under achievable practical conditions, that is using good quality connectors and central launching technique, the impact of modal noise on the system's performance, including nonlinearities, is expected to be low [19]. Under these conditions, the experimental results reported in [23] for the transmission of high-frequency subcarrier multiplexed CATV channels under linear intensity modulation can provide a good indication, as PM is inherently linear. These results showed that the CSO and CTB penalty due to MMF transmission yield values in the range of 3 to 7 dB.

By optimizing both the modulator and the detector responses for frequencies up to 30 GHz and reducing the channel spacing down to 100 MHz, a total of 240 data channels can be allocated in the operative spectrum region comprised between 6 and 30 GHz. In consequence, and assuming a linear capacity  $\times$  distance product typical of few mode MMF links, a potential aggregate bit rate per length product of 144 Gb/s $\cdot$ km could be achieved for the 5 km MMF link under evaluation. For that purpose, nonlinearities due to potential saturation of the detector arising from high peak-to-average power ratio would need to be bounded. A feasible technique could be that which is currently implemented to avoid clipping in direct-modulation laser based CATV systems by independently randomizing the initial phase of each subcarrier channel.

#### 4. Conclusions

A broadband phase-modulated MMF link has been successfully demonstrated for the first time to our knowledge by subcarrier transmission of high-frequency digital passband channels for bit rates up to 120 Mb/s. A cost-effective solution is presented in which a simple demodulation process is accomplished taking advantage of the phase-to-intensity conversion characteristic of a 5-km-length dispersive fiber link. The combination of the central launching technique and the use of low linewidth lasers contributed to the demonstrated capability of ROF transmission well beyond the typical MMF bandwidth-distance.

A satisfactory EVM was measured for subcarrier channels placed above 6 GHz for QPSK, 16-QAM and 64-QAM modulation formats. The total transmission capacity of the proposed phase-modulated MMF link can be enhanced by accommodating more passband channels in the phase-to-intensity-conversion operative frequency range and by combining the proposed subcarrier multiplexed approach with wavelength division multiplexing techniques.

#### Acknowledgments

The authors wish to acknowledge the financial support given by the Research Excellency Award Program GVA PROMETEO 2008/092.